

# Understanding Size Effects in the Advanced Through-Silicon Via Interconnect Schemes for 3D ICs

Imran Ali<sup>1</sup>, Ihor Radchenko<sup>1</sup>, Sasi Kumar Tippabhotla<sup>1</sup>, Song Wenjian M. Ridhuan<sup>1</sup>, Andrew A. O. Tay<sup>1</sup>, Nobumichi Tamura<sup>2</sup>, Seung Min Han<sup>3</sup>, Arief Suriadi Budiman<sup>1,\*</sup>

<sup>1</sup>SUTD Singapore University of Technology and Design, Singapore

<sup>2</sup>Advanced Light Source (BL 12.3.2), LBNL, Berkeley, CA, USA

<sup>3</sup>Graduate School of Energy, Environment, Water and Sustainability, Korea Advanced Institute of Science & Technology, Korea.

\*Corresponding author, [asbudiman@sutd.edu.sg](mailto:asbudiman@sutd.edu.sg)

## Abstract

Synchrotron X-ray microdiffraction has been successfully used to unravel how stresses evolve both in Cu through silicon via (TSV) as well as in silicon surrounding it. These findings have led to much improvements in solving the integration issues (pop-up/bulging of TSV during annealing, silicon delamination/fracture, etc.) as well as enhancing reliability and performance (reducing the “keep-away zone.”) in the microelectronics devices in the last 5 years. However, today’s microelectronics world has moved further into smaller and smaller technology nodes including the TSV diameters and pitches. This report will describe some of our most recent findings on the systematic studies of size effects using TSV samples fabricated with all the same fabrication methodology provided by SK Hynix, Inc. with diameters  $2\mu\text{m}$ ,  $5\mu\text{m}$  and  $8\mu\text{m}$ . Our investigation showed the smaller the TSV diameters, the stress is not necessarily the smaller and thus suggested that such smaller technology could lead to further integration issues and potentially reliability and performance concerns.

## Introduction

Three dimensional (3D) integrate circuit packaging technologies attract more attention because of progress in development of vertical interconnects, like through-silicon via (TSV) [1]. Despite potential benefits of TSVs in 3D packaging and integrated devices, their fabrication processes and integration still face several electrical and mechanical reliability challenges. Some of reliability issues are the result of residual thermal stress generated during manufacturing, testing, integration process steps, and operation of the TSV structures [2-3]. Stresses in the TSVs and close to active electronic devices/components are important since it can affect the electrical performance of stress-sensitive devices adjacent to the TSVs [4-5].

Stresses in Cu TSV also depend on Cu dimensions [6]. It was expected that lower diameter of TSV would have lower stresses [7]. However, the reported predictions did not take into account the microstructure of Cu TSV which may play a critical role for TSV diameters below  $5\mu\text{m}$  when the Cu grain sizes become comparable with TSV diameter [1].

In this study we will investigate effect of diameter on deviatoric stresses in Cu TSV as well as surrounding silicon after fabrication and annealing using synchrotron X-ray microdiffraction ( $\mu\text{SXR}$ D).

## Experimental Setup

Synchrotron X-ray microdiffraction has been used to measure stresses in Cu TSV. The  $\mu\text{SXR}$ D technique was developed at the Advanced Light Source, Berkeley Lab. The

technique can provide local information about the crystal structure of materials in a microscale. This became possible due to the focusing of X-rays into a micron size spot. The analysis of the obtained X-ray diffraction patterns allow to find and quantify not only the crystal structure and lattice parameters, but also the density of geometrically necessary dislocation density, crystal bending, polygonization and rotation, and local stress/strain probing at different conditions [8]. Further details about  $\mu\text{SXR}$ D have been described thoroughly elsewhere [9-13]. The  $\mu\text{SXR}$ D experiment was conducted at the Beamline at the Advanced Light Source (ALS), Lawrence Berkeley National Laboratory (LBNL). We have studied deviatoric stress evolution in Cu TSV and surrounding silicon using  $\mu\text{SXR}$ D. The simplified experimental setup diagram is shown in Fig. 1(c). Incoming X-ray beam illuminate a volume that may consist of more than one crystal, the diffracted beams from each of the crystal are captured by the CCD detector placed above the sample.

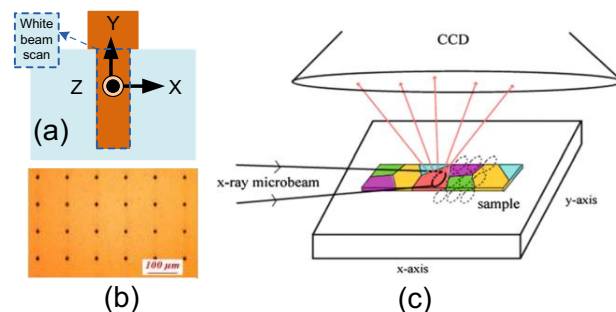


Fig. 1. Experimental setup, used to study stress in Cu TSV. (a) Cross-section view of Cu TSV showing white beam scan region and schematic of the coordinate system used to calculate deviatoric stresses. (b) Optical micrograph, showing the top view of Cu TSV sample where dark spots correspond to TSVs. (c) Experimental setup of a  $\mu\text{SXR}$ D. Incoming X-ray beam illuminate a volume that may consist of more than one crystal, the diffraction pattern from each of the crystal are captured by the CCD detector placed above the sample. Laue patterns are collected from each discrete volume of the sample [14].

In our experiment the white-beam (polychromatic) X-rays were used to enable measurements of deviatoric components of the stress tensor. The sample was mounted on a precision XY stage and the anode point was scanned under the focused X-ray beam as shown in Fig. 1(c). The focused X-ray beam size was  $1 \times 1 \mu\text{m}$  (full-width at half-max intensity). The energy range of 5-25keV has been used for white beam X-rays. The TSV samples were fabricated with all the same fabrication

methodology provided by SK Hynix, Inc. The Cu TSVs were assembled in an array with  $100\mu\text{m}$  pitch. The schematic of top view of Cu TSV is shown in Fig. 1(b). Samples were prepared by electroplating and annealed at  $100^\circ\text{C}$  and  $400^\circ\text{C}$ . After annealing the samples were polished from the top and along the cross-section to allow X-rays penetration into Cu through surrounding Si. The details of sample preparations were described in details elsewhere [5]. The white beam scan was performed over one of the TSV in each of three samples using  $0.5\mu\text{m}$  step size with white beam of  $1\mu\text{m}$  diameter [10]. The schematic of TSV and white beam scan region is also shown in Fig. 1(a). The deviatoric stress components of Cu TSV and surrounding silicon were studied using  $2\mu\text{m}$ ,  $5\mu\text{m}$  and  $8\mu\text{m}$  diameter of Cu TSV.

## Results and Discussion

Figs. 2-7 show stress components of all deviatoric stresses (normal as well as shear) and their distribution across TSV.

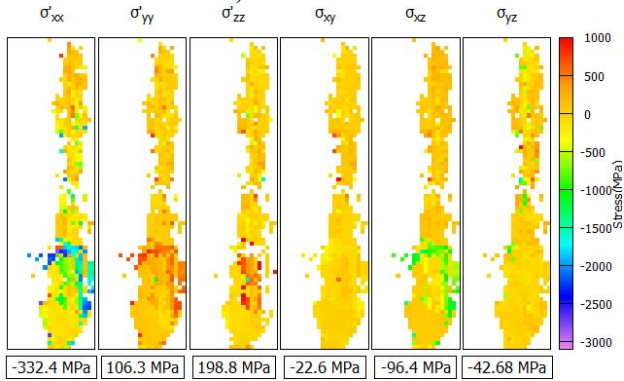


Fig. 2. White beam diffraction results for  $2\mu\text{m}$  diameter of Cu TSV. The deviatoric stress in Cu after annealing at  $400^\circ\text{C}$ . The average stresses shown below each stress maps are calculated by averaging all stresses in each pixel. The pixel sizes for all stress maps are  $0.5 \times 0.5\mu\text{m}$ .

The deviatoric stress distribution in  $2\mu\text{m}$  diameter of Cu is illustrated on Fig. 2. The stress maps show all components of deviatoric stresses (normal and shear) and their distribution across TSV domain. The normal deviatoric stresses  $\sigma'_{xx}$ ,  $\sigma'_{yy}$  and  $\sigma'_{zz}$  are full normal stresses ( $\sigma_{xx}$ ,  $\sigma_{yy}$  and  $\sigma_{zz}$ ) without hydrostatic components. Whereas  $\sigma_{xy}$ ,  $\sigma_{xz}$  and  $\sigma_{yz}$  are full deviatoric shear stresses. The average of normal deviatoric stress components in  $2\mu\text{m}$  diameter of Cu TSV is  $-9\text{MPa}$ , while the average shear stress component is  $54\text{MPa}$ . The stress maps of  $2\mu\text{m}$  diameter Cu TSV show that  $\sigma'_{xx}$  normal deviatoric stress component is highly compressive ( $-332\text{MPa}$ ) while  $\sigma'_{zz}$  is under high tensile deviatoric stresses. When there is high normal compressive stress in  $\sigma'_{xx}$  direction in smaller diameter ( $2\mu\text{m}$ ) of Cu TSV then these high compressive stresses will cause Cu TSV to expand in  $\sigma'_{yy}$  and  $\sigma'_{zz}$  direction. Which is may be one of the reason that  $\sigma'_{zz}$  ( $198.8\text{MPa}$ ) and  $\sigma'_{yy}$  ( $106.3\text{MPa}$ ) are higher. The deviatoric shear stress component  $\sigma_{xz}$  ( $-96\text{MPa}$ ) is higher than  $\sigma_{xy}$  and  $\sigma_{yz}$  ( $-22.6\text{MPa}$  and  $-42.68$ ). This is may be because our sample was polished

in Y-direction and Z-direction which made shear deviatoric stress components of  $\sigma_{xy}$  and  $\sigma_{yz}$  more relaxed.

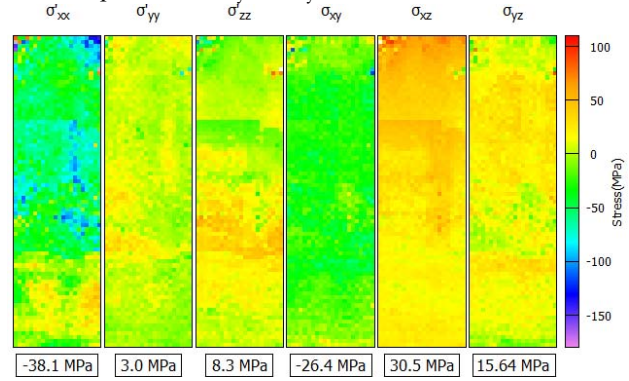


Fig. 3. White beam diffraction results for silicon surrounding  $2\mu\text{m}$  diameter Cu TSV. The deviatoric stress in silicon surrounding Cu after annealing at  $400^\circ\text{C}$  is shown. The average stresses shown below each stress maps are calculated by averaging all stresses in each pixel. The pixel sizes for all stress maps are  $0.5 \times 0.5\mu\text{m}$ .

The deviatoric stress distribution in silicon surrounding  $2\mu\text{m}$  diameter of Cu TSV is illustrated on Fig. 3. The average normal component of the deviatoric stress is  $-8.9\text{MPa}$ , while the average shear deviatoric stress component is  $6.6\text{MPa}$ . The average deviatoric stresses in silicon is lower than Cu. There could be couple of reasons of stresses in Cu and surrounding silicon in TSV, such as diameter of Cu TSV and coefficient of thermal mismatch (CTE) between Cu and silicon. The growth of grains in Cu TSV may be also one of reasons of high stresses in Cu. As grains grows in Cu during thermal annealing and at room temperature causing additional tensile stress in Cu [5]. High stresses in Cu TSV may cause delamination and fracture in Cu TSV. The high stresses in silicon will introduce keep-away zone and also leads to device performance and reliability issues.

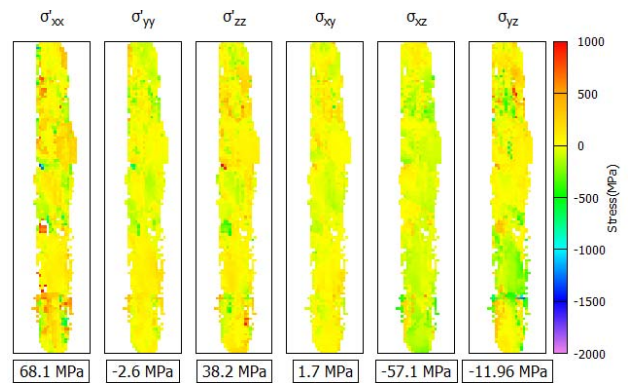


Fig. 4. White beam diffraction results for  $5\mu\text{m}$  diameter of Cu TSV. The deviatoric stress in Cu after annealing at  $400^\circ\text{C}$ . The average stresses shown below each stress maps are calculated by averaging all stresses in each pixel. The pixel sizes for all stress maps are  $0.5 \times 0.5\mu\text{m}$ .

The deviatoric stress distribution in  $5\mu\text{m}$  diameter of Cu is illustrated on Fig. 4. The average of normal deviatoric stress components of  $5\mu\text{m}$  diameter TSV is  $34.6\text{MPa}$  which is higher than  $2\mu\text{m}$  TSV sample ( $-9\text{MP}$ ) but individual components of normal deviatoric stresses ( $\sigma'_{xx}$ ,  $\sigma'_{yy}$  and  $\sigma'_{zz}$ ) in  $2\mu\text{m}$  diameter TSV sample are higher than  $5\mu\text{m}$  diameter TSV sample. The average shear stress component  $5\mu\text{m}$  is  $-22.5\text{MPa}$  whose magnitude is approximately twice lower than  $2\mu\text{m}$  diameter of Cu TSV. The stress maps of  $5\mu\text{m}$  diameter Cu TSV show that  $\sigma'_{yy}$  normal deviatoric stress component is compressive ( $-2.6\text{MPa}$ ) while  $\sigma'_{xx}$  and  $\sigma'_{zz}$  ( $68.1\text{MPa}$  and  $38.2\text{MPa}$ ) are under high tensile deviatoric stresses.

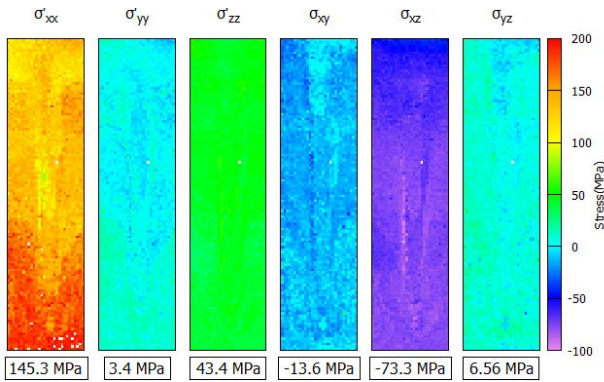


Fig. 5. White beam diffraction results for silicon surrounding  $5\mu\text{m}$  diameter Cu TSV. The deviatoric stress in silicon surrounding Cu after annealing at  $400^\circ\text{C}$  is shown. The average stresses shown below each stress maps are calculated by averaging all stresses in each pixel. The pixel sizes for all stress maps are  $0.5 \times 0.5\mu\text{m}$ .

The deviatoric stress distribution in silicon surrounding  $5\mu\text{m}$  diameter of Cu TSV is illustrated on Fig. 5. The average normal component of the deviatoric stress is  $64\text{MPa}$ , while the average shear stress component is  $-26.8\text{MPa}$ . For  $5\mu\text{m}$  diameter Cu TSV the deviatoric normal stresses in silicon ( $64\text{MPa}$ ) are higher than deviatoric normal stresses in Cu ( $34.6\text{MPa}$ ). Whereas magnitude of average deviatoric shear stresses in silicon surrounding Cu TSV ( $-26.5\text{MPa}$ ) are more compressive than deviatoric shear stresses in Cu TSV ( $-22.5\text{MPa}$ ). The magnitude of average deviatoric normal stresses ( $64\text{MPa}$ ) in silicon surrounding  $5\mu\text{m}$  diameter are higher than average deviatoric normal stresses ( $-8.9\text{MPa}$ ) in silicon surrounding  $2\mu\text{m}$  diameter Cu TSV.

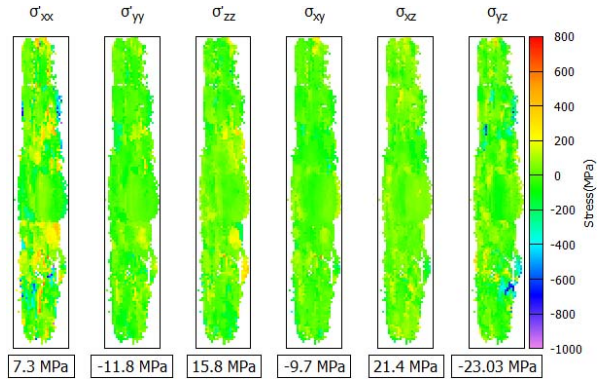


Fig. 6. White beam diffraction results for  $8\mu\text{m}$  diameter of Cu TSV. The deviatoric stress in Cu after annealing at  $400^\circ\text{C}$ . The average stresses shown below each stress maps are calculated by averaging all stresses in each pixel. The pixel sizes for all stress maps are  $0.5 \times 0.5\mu\text{m}$ .

The deviatoric stress distribution in  $8\mu\text{m}$  diameter of Cu is illustrated on Fig. 6. The average normal component of the deviatoric stress is  $3.8\text{MPa}$  which is lower in magnitude than  $2\mu\text{m}$  sample ( $-9\text{MP}$ ) and  $5\mu\text{m}$  sample ( $34.6\text{MPa}$ ). The average shear stress magnitude is  $-3.8\text{MPa}$  which is also lower than  $2\mu\text{m}$  TSV sample ( $6.6\text{MPa}$ ) and  $5\mu\text{m}$  sample ( $-22.5\text{MPa}$ ).

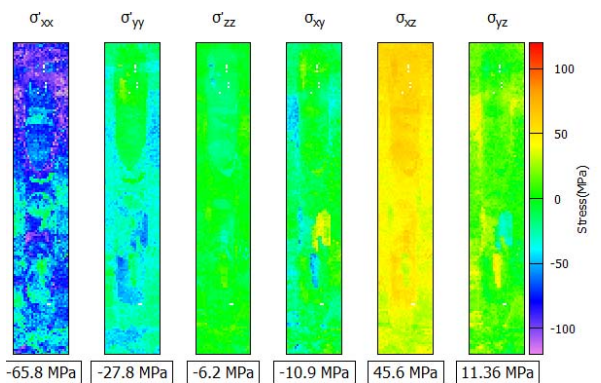


Fig. 7. White beam diffraction results for silicon surrounding  $8\mu\text{m}$  diameter Cu TSV. The deviatoric stress in silicon surrounding Cu after annealing at  $400^\circ\text{C}$  is shown. The average stresses shown below each stress maps are calculated by averaging all stresses in each pixel. The pixel sizes for all stress maps are  $0.5 \times 0.5\mu\text{m}$ .

The deviatoric stress distribution in silicon surrounding  $8\mu\text{m}$  diameter of Cu TSV is illustrated on Fig. 7. The average normal component of the deviatoric stress is  $-33.3\text{MPa}$ , while the average shear stress component is  $15.4\text{MPa}$ . The average magnitude of deviatoric stresses (normal as well as shear) in silicon surrounding Cu TSV of diameter  $8\mu\text{m}$  are higher than in silicon surrounding Cu TSV of diameter  $2\mu\text{m}$  and lower than  $5\mu\text{m}$  Cu TSV. The Cu TSV diameter is also one of the factor affect stresses in silicon. Further studies are required to find more suitable diameter with less stresses.

## Conclusions

Synchrotron X-ray microdiffraction has been used to unravel how stresses evolve both in Cu TSV as well as in the silicon surrounding it. These findings have led to much improvements in solving the integration issues (pop-up/bulging of TSV during annealing, silicon delamination/fracture, etc.) as well as enhancing reliability and performance (reducing the “keep-away zone.”) in the microelectronics devices in the last 5 years. In this report we have described some of our most recent findings on the systematic studies of size effects using TSV samples fabricated with all the same fabrication methodology provided by SK Hynix, Inc. with three different diameters, ie.  $2\mu\text{m}$ ,  $5\mu\text{m}$  and  $8\mu\text{m}$ . Our investigation showed the smaller the TSV diameters, the stress is not necessary the smaller. Thus it is suggested that such smaller technology could lead to further integration issues and potentially reliability and performance concerns.

## Acknowledgments

The authors gratefully acknowledge collaborations with SK Hynix, Inc. in Korea providing samples and special thank to Singapore University of Technology and Design (SUTD) scholarship. The Advanced Light Source (ALS) is supported by the Director, Office of Science, Office of Basic Energy Sciences, of the U.S. Department of Energy under Contract No. DE-AC02-05CH11231 at the Lawrence Berkeley National Laboratory (LBNL).

## References

1. H.A.-S. Shin, B.-J. Kim, J.-H. Kim, S.-H. Hwang, A.S. Budiman, H.-Y. Son, et al., “Microstructure Evolution and Defect Formation in Cu Through-Silicon Vias (TSVs) During Thermal Annealing,” *J. Electron. Mater.* 41 (2012) 712–719.
2. T. Jiang, S.-K. Ryu, Q. Zhao, J. Im, R. Huang, et al., “Measurement and analysis of thermal stresses in 3D integrated structures containing through-silicon-vias,” *Microelectron. Reliab.* 53 (2013) 53–62.
3. L.W. Schaper, S.L. Burkett, S. Spiesshoefer, G.V. Vangara, et al., “Architectural implications and process development of 3-D VLSI Z-axis interconnects using through silicon vias,” *IEEE Trans. Adv. Packag.* 28 (2005) 356–366.
4. S.-K. Ryu, T. Jiang, K.H. Lu, J. Im, H.-Y. Son, K.-Y. Byun, et al., “Characterization of thermal stresses in through-silicon vias for three-dimensional interconnects by bending beam technique”, *Appl. Phys. Lett.* 100 (2012) 041901–041904.
5. Budiman, A. S., H.-A.-S. Shin, B.-J. Kim, S.-H. Hwang, H.-Y. Son, M.-S. Suh, Q.-H. Chung et al. “Measurement of stresses in Cu and Si around through-silicon via by synchrotron X-ray microdiffraction for 3-dimensional integrated circuits”, *Microelectronics Reliability* 52, no. 3 (2012): 530-533.
6. Liu, Xi, et al. “Experimental Stress Characterization and Numerical Simulation for Copper Pumping Analysis of Through-Silicon Vias”, *IEEE TRANSACTIONS ON COMPONENTS, PACKAGING AND MANUFACTURING TECHNOLOGY*, VOL. 6, NO. 7, JULY 2016.
7. Lu, Kuan Hsun, Suk-Kyu Ryu, Qiu Zhao, Rui Huang, and Paul S. Ho. “Interfacial Delamination Between Through Silicon Vias (TSVs) and Silicon Matrix”, In *ASME 2010 International Mechanical Engineering Congress and Exposition*, pp. 105-112. American Society of Mechanical Engineers, 2010.
8. A.S. Budiman, “Probing plasticity at small scales: From electromigration in interconnects to dislocation hardening processes in crystals”, PhD dissertation, *Stanford University, Palo Alto, CA* (2008)
9. MacDowell, A. A., R. S. Celestre, Nobumichi Tamura, Ralph Spolenak, Bryan Valek, W. L. Brown, J. C. Bravman, H. A. Padmore, B. W. Batterman, and J. R. Patel. “Submicron X-ray diffraction”, *Nuclear Instruments and Methods in Physics Research Section A: Accelerators, Spectrometers, Detectors and Associated Equipment* 467 (2001): 936-943.
10. Tamura, N., A. A. MacDowell, R. Spolenak, B. C. Valek, J. C. Bravman, W. L. Brown, R. S. Celestre, H. A. Padmore, B. W. Batterman, and J. R. Patel. “Scanning X-ray microdiffraction with submicrometer white beam for strain/stress and orientation mapping in thin films”, *Journal of Synchrotron Radiation* 10, no. 2 (2003): 137-143.
11. Van Swygenhoven, H., B. Schmitt, P. M. Derlet, S. Van Petegem, A. Cervellino, Z. Budrovic, S. Brandstetter, A. Bollhalder, and M. Schild. “Following peak profiles during elastic and plastic deformation: A synchrotron-based technique”, *Review of scientific instruments* 77, no. 1 (2006): 013902.
12. Valek, Bryan Charles, “X-ray microdiffraction studies of mechanical behavior and electromigration in thin film structures”, 2003.
13. Tamura, N., R. S. Celestre, A. A. MacDowell, H. A. Padmore, R. Spolenak, B. C. Valek, N. Meier Chang, A. Manceau, and J. R. Patel. “Submicron x-ray diffraction and its applications to problems in materials and environmental science”, *Review of scientific instruments* 73, no. 3 (2002): 1369-1372
14. Budiman, Arief Suriadi, “Probing crystal plasticity at the nanoscales: Synchrotron X-ray microdiffraction”, *Springer*, 2015.